1

# MASTER

BNL-27495     CONF-800624--1

## NSLS DIPOLE POWER SOURCE*

Gregory P. Bagley

National Synchrotron Light Source
Brookhaven National Laboratory, Upton, New York 11793

### ABSTRACT

An SCR DC to DC converter is described which
will operate at an output of 275 kW and will supply
current to electron storage ring magnets requiring
5 hr. stability of 50 ppm. The operation of this
modified chopper is described and design equations
are presented, along with the system control loop
description.

## INTRODUCTION

The National Synchrotron Light Source (NSLS)
under construction at Brookhaven Laboratory will be
a uniquely copious source of x-ray and ultraviolet
photons with a wide spectrum. Selected frequencies
of this radiation with wavelengths of the order of
atomic and molecular dimensions will be an impor-
tant tool in the study of matter. Some of the
potential uses of this light include studies of
absorption spectra, photo emission of electrons,
x-ray scattering, biochemical studies and other
areas of basic research. It can also be used for
micro-lithography of integrated circuits for
ultra-dense semiconductor devices.

This light is generated by electrons which are
made to follow a closed orbit in an electron stor-
age ring at nearly the speed of light in vacuum
thus undergoing centripetal acceleration due to the
magnetic guide field. This acceleration causes the
electron beam to radiate energy with a wide spec-
trum with a peak dependent on the electron energy
and the radius of curvature. The NSLS will include
two electron storgage rings; one operating at an
energy of 0.7 GeV with a peak or characteristic
wavelength in the vacuum ultraviolet (VUV) region,
the other at 2.5 GeV with a characteristic wave-
length in the soft x-ray region. The beam storage
duration is dependent on the mutual repulsion of
the electronic charges, collisions with the resid-
ual gas in the vacuum and the stability of the
magnetic field of the storage ring dipoles, among
other things[1,2].

## DESIGN REQUIREMENTS

The power source required for the storage
ring dipoles of the National Synchrotron Light
Source must meet a number of stringent require-
ments. It must generate a nominal 1500A at 65Vdc
for the VUV ring (or 185Vdc for the x-ray ring)
with a relatively slow rise and decay and with a
short term (5 hr.) current stability of ± 50 ppm,
max in order to maintain the beam orbit within
desired limits. The required long term stability
is ± 100 ppm, max, over one month. The peak to
peak magnetic field ripple must be less than 50
ppm. Thus the power source must be virtually
independent of the 480V, 3∅, 60 Hz line voltage
variations, phase imbalances and transformer/recti-
fier tolerances. Also a ± 10° temperature varia-
tion at the power supply must be anticipated.

### Design Alternates

Phase controlled SCR approaches with various
correction circuits to minimize the effects of line
voltage perturbations and line frequency variations
as well as the transistor bank regulator approach
were considered. The problem of sensing the line
voltage zero crossing of the SCR phase controlled
regulator in the presence of frequency variations
can be solved with a phase locked loop but line
voltage perturbations can only be corrected by
shifting of the subsequent SCR trigger. The re-
sulting wobble in the regulator output is attenu-
ated but not eliminated by the filtering of the
inductive magnet load.

The transistor bank regulator can produce
relatively fast responses to disturbances. The
inefficiency of the transistor bank regulator can
be minimized by different preregulator approaches
which add to its complexity and cost. It is an
expensive approach but it is capable of wideband,
effective control.

A cheaper, more energy efficient alternate is
an SCR switching regulator or chopper. When used
in a type 1, 100 Hz bandwidth loop with feedforward
control to correct for input voltage variations,
the chopper loop has adequate control agility for
the storage ring application while eliminating
virtually all the variations and imperfections of
the input a.c. power source. The chopper approach
which was chosen is based on a voltage commutated
chopper described by Dewan and Jackson because it
permits more rapid turnoff of the series switch at
the instant required by the loop control. It re-
sults in a straight forward single input-single
output control system which meets the design goals

## DISCLAIMER

This report was prepared as an account of work sponsored by an agency of the United States Government. Neither the United States Government nor any agency Thereof, nor any of their employees, makes any warranty, express or implied, or assumes any legal liability or responsibility for the accuracy, completeness, or usefulness of any information, apparatus, product, or process disclosed, or represents that its use would not infringe privately owned rights. Reference herein to any specific commercial product, process, or service by trade name, trademark, manufacturer, or otherwise does not necessarily constitute or imply its endorsement, recommendation, or favoring by the United States Government or any agency thereof. The views and opinions of authors expressed herein do not necessarily state or reflect those of the United States Government or any agency thereof.

# DISCLAIMER

**Portions of this document may be illegible in electronic image products. Images are produced from the best available original document.**

without significant complications or cost.

## Chopper Operation (See Figure 1)

Basically the chopper operates as follows:

The load switch turn-on occurs as a direct result of the clock pulse, connecting the input voltage source to the output filter and load. Turn-off occurs as a result of the comparison of the integral of the load switch output $v_s$, and the amplified error voltage. The OFF switch (Q2) is then triggered connecting the load switch anode (Q1) to the negatively charged commutating capacitor, C, forcing the load switch off. This is followed by a flyback and recovery sequence which ends with the C again charged negatively to ground.

After the contactor closes, the sequence must begin with the inhibit of triggers by the triggering logic until the input filter capacitor, Cl, is charged. A series of OFF triggers is then generated each of which starts a flyback and recovery sequence which proceeds as follows:

Q2 is triggered causing C to charge to 2v thru Ll. The gate of Q3 is held off by the current in the diode, D2, although Q3 is forward biased. After that first 1/2 sine of current thru Q2 and D2 ceases, Q3 conducts, resulting in a second 1/2 sine of current thru C and L4 and a reversal of the voltage on C.

Assuming no losses and Ll = L2, on subsequent triggers, C, initially charged to -2v, will tend to charge to + 4v. However, D1 begins conducting when the voltage induced in L2, which is tightly coupled to Ll, equals +v, thus tending to clamp the voltage on C to + 2v. The current in Q2 then decreases to zero, disconnecting C and Ll. The current thru D1 then decreases to zero, while returning energy to Cl and discharging the L1/L2 transformer while the C voltage again returns to - 2v as a result of recovery current thru Q3 and L4.

The triggering logic then permits the load switch, Q1, to be triggered by the ON pulse, charging Ll. The loop generated trigger pulse to Q2 later turns off Q1 by forcing the anode of Q1 negative long enough to allow charge recombination in Q1 so that Q1 will remain off (up to 25 sec for the presently used units). During the OFF period, load current continues to flow thru D3. The flyback proceeds as before except that the initial current in Ll adds to the initial energy in Ll and results in the minimum time for Q1 charge recombination.

The output filter with a resonant frequency of 400 Hz attenuates the high frequency components of the resulting square at the junction of Q1 and D3. The VUV dipole load magnet, with a time constant of 2.07 sec (x-ray, 2.6 sec), further reduces the ripple component of the current to acceptable levels.

## CIRCUIT EQUATIONS SUMMARY

As the equivalent circuit and waveforms of figure 2 indicate, the steady state current thru L5 changes linearly in the two regions, $\tau_1$ and $\tau_2$. The change in current in L5 is given by

$$I_2 - I_1 = \frac{v - v_o}{L_1 + L_5}\tau_1 \text{ and } I_2 - I_1 = \frac{v_o}{L_5}\tau_2$$

The average output current, $I_o$, is then

$$I_o = \frac{I_1 + I_2}{2}$$

With $\tau_1 + \tau_2 = T$, if follows that the peak current in $Q_2$, $I_2$, is

$$I_2 = I_o + \frac{T/2}{\frac{L_1 + L_5}{v - v_o} + \frac{L_5}{v_o}} \tag{1}$$

At $t_2$ the OFF SCR is triggered with a rapid turnoff of Q1. Then the current thru $L_1$, i, is found from

$$v = L_1\frac{di}{dt} + \frac{1}{C}\int i \, dt : i(0) = I_2, v_c(0) = v_{co}, t = 0@t_2$$

or

$$\frac{v}{s} = L_1\left(sI(s) - I_2\right) + \frac{1}{C}\left(\frac{I(s)}{s} + \frac{Cv_{co}}{s}\right). \text{ Then}$$

$$I(s) = \frac{(v - v_{co})/L_1 + sI_2}{s^2 + \frac{1}{L_1 C}},$$

or

$$i(t) = I_2\cos\omega_o t + (v - v_{co})\sqrt{\frac{C}{L_1}}\sin\omega_o t$$

where $\omega_o = 1/\sqrt{L_1 C}$. $\tag{2}$

Now

$$v_c(t) = v - L_1\frac{di}{dt} = v + \sqrt{\frac{L_1}{C}}I_2\sin\omega_o t - (v - v_{co})\cos\omega_o t \tag{3}$$

Q1 is reverse biased for the period, $t_q$, which is found when $v_c(t_q) = 0$.

Then

$$t_q = \frac{1}{\omega_o}\left[\cos^{-1}\left(\frac{v^2}{\frac{L_1}{C}I_2^2 + (v - v_{co})^2}\right)^{\frac{1}{2}} - \tan^{-1}\left(\frac{I_2\sqrt{\frac{L_1}{C}}}{v - v_{co}}\right)\right].$$

Given $I_2$ and v, $L_1$ and C are chosen such that $t_q$ is always greater than the turn off time of Q1. See Dewan[3].

$I_3$, the peak value of $i$, occurs at $t_3$ when $v_c(t_3-t_2) = v$. From (3)

$$t_3 - t_2 = \frac{1}{\omega_0} \tan^{-1}\left(\frac{v - v_{co}}{I_2\sqrt{L_1/C}}\right),$$

and from (2)

$$I_3 = \left[I_2^2 + \frac{C}{L_1}(v - v_{co})^2\right]^{\frac{1}{2}}.$$

The increasing voltage of $v_A (= v_c)$ induces a decreasing voltage across D1 via M until D1 is forward biased. That point is reached when $v = -M\frac{di}{dt}$ or $\frac{di}{dt} = -\frac{v}{M}$. Then from (3)

$$v_c(t_4-t_2) = v-L_1\frac{di}{dt} = v\left(1 + \frac{L_1}{M}\right)$$

or

$$v\left(1+\frac{L_1}{M}\right) = v+I_2\sqrt{\frac{L_1}{C}}\sin\omega_0(t_4-t_2)$$
$$- (v-v_{co})\cos\omega_0(t_4-t_2).$$

Thus

$$t_4-t_2 = \frac{1}{\omega_0}\left[\cos^{-1}\left(\frac{-\frac{L_1}{M}v}{\left[\frac{L_1}{C}I_2^2+(v-v_{co})^2\right]^{\frac{1}{2}}}\right)\right.$$
$$\left. - \tan^{-1}\left(\frac{I_2\sqrt{\frac{L_1}{C}}}{v - v_{co}}\right)\right]$$

and

$$I_4 = i(t_4-t_2) = I_2\cos\omega_0(t_4-t_2)$$
$$- (v-v_{co})\sqrt{\frac{C}{L_1}}\sin\omega_0(t_4-t_2).$$

When D1 conducts, returning energy to V, the following equations apply where $i_1$ is the current thru $L_1$ and C, $i_2$ is the forward current in D1 and L2. The lead inductance, $\ell$, must also be included:

$$v = \ell\frac{d}{dt}(i_1-i_2) + L_1\frac{di_1}{dt} + \frac{1}{C}\int i_1 dt + M\frac{di_2}{dt}$$

$$-v = \ell\frac{d}{dt}(i_2-i_1) + L_2\frac{di_2}{dt} + M\frac{di_1}{dt}$$

where $t = 0$ @ $t_4$, $i_1(0) = I_4$ and $v_c(0) = v\left(1+\frac{L_1}{M}\right)$. In the s plane,

$$(\ell+L_1)I_4 - \frac{v}{s}\frac{L_1}{M} = I_1(s)\left[s(\ell+L_1) + \frac{1}{sC}\right]$$
$$+ I_2(s)\left[s(M - \ell)\right]$$

$$(M-\ell)I_4 - \frac{v}{s} = I_1(s)\left[s(M-\ell)\right] + I_2(s)\left[s(L_2+\ell)\right]$$

from which

$$I_1(s) = \frac{sI_4 - \frac{v}{L_e}\left(\frac{L_1}{M} + \frac{\ell-M}{\ell+L_2}\right)}{s^2 + \omega_1^2}$$

and $I_2(s) =$

$$\frac{-s^2\frac{v}{L_e}\frac{\ell\left(\frac{L_1}{M}+1\right)}{(\ell+L_2)} + sI_4\frac{M-\ell}{CL_e(\ell+L_2)} - \frac{v}{CL_e(\ell+L_2)}}{s^2\left[s^2 + \omega_1^2\right]}$$

where

$$\omega_1 = \frac{1}{\sqrt{CL_e}} \text{ and } L_e = \frac{\ell(L_1+L_2+2M) + L_1L_2 - M^2}{\ell + L_2}.$$

Then

$$i_1(t) = I_4\cos\omega_1 t - v\sqrt{\frac{C}{L_e}}\left(\frac{L_1}{M} + \frac{\ell-M}{\ell+L_2}\right)\sin\omega_1 t \text{ and}$$

$$i_2(t) = v\sqrt{\frac{C}{L_e}}\left(\frac{L_e-\ell\left(1+\frac{L_1}{M}\right)}{L_2 + \ell}\right)\sin\omega_1 t - \frac{v}{L_2+\ell}t$$
$$+ \frac{I_4(M-\ell)}{L_2 + \ell}(1 - \cos\omega_1 t).$$

At Q2 turn-off,

$$i_1(t_5-t_4) = 0 \text{ or } t_5-t_4 = \frac{1}{\omega_1}\tan^{-1}\left[\frac{\frac{I_4}{v}\sqrt{\frac{L_e}{C}}}{\frac{L_1}{M} + \frac{\ell-M}{\ell+L_2}}\right]$$

and $i_2(t_5-t_4) \equiv I_5$

The final capacitor voltage is then

$$v_c(t_5-t_4) = v\left(1 + \frac{L_1}{M}\right) + \frac{1}{C}\int_0^{t_5-t_4} i_1 dt$$

$$v_c(t_5-t_4) = I_4\sqrt{\frac{L_e}{C}}\sin\omega_1(t_5-t_4)$$

$$+v\left[1+\frac{M-\ell}{L_2+\ell}+\left(\frac{L_1}{M}-\frac{M-\ell}{L_2+\ell}\right)\cos\omega_1(t_5-t_4)\right].$$

After Q2 stops conducting $i_1 = 0$, $i_2 = I_5$, the simple first order equation in $i_2$ yields

$$t_6 = t_5 + \frac{I_5}{v}\frac{L_2+\ell}{v}$$

The preceding analysis does not include core loss and copper loss in the coils or losses in the capacitors. These losses will result in lower peaks in the maximum $v_c$ and $i_{Q2}$. However, in the case of the circuit of figure 1 which shows one of two chopper switches which are switched on alternately, $L_1 = L_2 = 20uhy$, $C = 100uf$, $L_5 = 75uhy$, $v = 200Vdc$, $v_{co} = 500v$ $M = 19uhy$, $\ell = 1uhy$, $v_o = 70v$ and $I_o = 750A$.

Then

| I | | $v_c$, $v_A$ | |
|---|---|---|---|
| $I_1 = 556A$ | | $v_{A1} = 173v$ | |
| $I_2 = 945A$ | | $v_{A2} = 173v$ | |
| $I_3 = 1830A$ | | | |
| $I_4 = 1780A$ | | $v_{c4} = v_{A4} = 400v$ | |
| $I_5 = 1190A$ | | $v_{c5} = v_{A5} = 793v$ | |

| t | | $\Delta t$ | |
|---|---|---|---|
| $t_1 = 55\mu sec$ | | $\tau_1 = t_2-t_1 = 280\mu sec$ | |
| $t_2 = 385\mu sec$ | | $t_q = 35\ \mu sec$ | |
| $t_3 = 431\mu sec$ | | $t_3-t_2 = 46\mu sec$ | |
| $t_4 = 442\mu sec$ | | $t_4-t_2 = 57\mu sec$ | |
| $t_5 = 477\mu sec$ | | $t_5-t_4 = 35\mu sec$ | |
| $t_6 = 602\mu sec$ | | $t_6-t_5 = 120\mu sec$ | |
| $T = 714\mu sec$ | | $\tau_2 = t_7-t_2 = 416\mu sec$ | |

## Feedforward Circuit

The system operates to keep the average value of switch output voltage, $v_3$, directly proportional to a control voltage on a pulse to pulse basis, virtually eliminating line variations. This is accomplished by applying a voltage proportional to the instantaneous value of the switch output voltage to an integrator. The output of the integrator is compared with the control voltage to generate the OFF pulse. See Figure 1. Variations in the line voltage, v, whether due to phase imbalance,

ripple or line perturbations are integrated to advance or retard the OFF pulse giving a feedforward correction to hold the average value of the switch output voltage proportional to the control voltage, $v_2$.

After being reset at $t_o = 0$ the integrator output is

$$v_1(t) = \frac{1}{R'C'}\int_0^t -\alpha v_3(t)\ dt = -\frac{\alpha}{R'C'}\int_0^t v_3(t)\ dt$$

The OFF trigger occurs at $t_2$ when $v_1(t_2) = -\frac{R_1}{R_2}v_2(t_2)$, after which $v_3 = 0$ until the next ON pulse occurs. The average value of $v_3$, $\bar{v}_3$, is then $\bar{v}_3 = \frac{1}{T}\int_0^{t_2}v_3(t)\ dt$. Thus $v_1(t_2) = -\frac{\alpha}{R'C'}T\bar{v}_3 = -\frac{R_1}{R_2}v_2(t_2)$ from which $\bar{v}_3$ is a linear function of $v_2(t_2)$:

$$\bar{v}_3 = -\frac{R_1 R'C'}{\alpha TR_2}v_2(t_2)$$

## Control Loop

The block diagram of Figure 3 includes the approximate low frequency transfer function of the load magnets and the linearization of the switch transfer discussed above. The current to be regulated is sensed by a precision Hazemeyer D.C. current transformer which is rated at $\pm 1$ ppm/°C gain temperature coefficient with an absolute accuracy of $\pm 10$ ppm of full scale. The output of the DCCT is compared with the output of a selected 16 bit D/A converter which has negligible offset variation and a gain T.C. of 2 ppm/°C max in a chopper stabilized precision error amplifier. The A2 integrator minimizes static loop gain errors and provides lead-lag compensation for loop stability. The resulting static errors should be within the time and temperature stability requirements.

The switch output filter will reduce the 1.4K & 2.8K Hz basic ripple and eliminate the higher harmonics of the chopper output. The inductance of the load magnets and the attenuation due to eddy currents in the magnet laminations and the aluminum vacuum chamber will further reduce the field ripple seen by the beam to acceptable levels.

The frequency response of the components of the system as well as the overall open loop gain and phase frequency response are given in Figure 4. Analytically,

$$GH = \left[ (R_D) \left( \frac{R_1 \left( 1 + \frac{s}{\omega_1} \right)}{sR_c C_1 \left( 1 + \frac{s}{\omega_j} \right)} \right) \left( -\frac{R_1 R' C'}{R_2 \, \alpha \, T} \right) \right.$$

$$\left. \left( \frac{1 + b \frac{s}{\omega_o}}{\left( 1 + c \frac{s}{\omega_o} \right) \left( 1 + 2\gamma a \frac{s}{\omega_o} + \left( \frac{as}{\omega_o} \right)^2 \right)} \right) \frac{1}{R \left( s \frac{L}{R} + 1 \right)} \right] \left[ \frac{r}{R_A} \right]$$

for which in the case of the 7UV dipoles,

| | |
|---|---|
| $R_D = 500K$ | $R_1 = 2K$ |
| $R_1 = 16K$ | $R_2 = 5.6K$ |
| $R_c = 2.4K$ | $R' = 51K$ |
| $C_1 = 1uf$ | $C' = .01uf$ |
| $C_j = .01uf$ | $\alpha = .05$ |

| | |
|---|---|
| $T = .7msec$ | $R = .044\Omega$ |
| $\omega_o = 628rps$ | $L = 91.5mhy$ |
| $a = .605$ | $r = 10v/2000A$ |
| $b = 1.6$ | $R_A = 5K$ |
| $c = .875$ | $\gamma = 0.6$ |

The phase margin at the gain crossover at 100 Hz is then 68° which results in optimum system speed of response and settling time.

## CONCLUSION

The design described meets the requirements for the system with an approach that reduces to a straight forward control loop. It avoids the complication of multiple correction loops required for an SCR phase control loop to achieve this level of stability or the cost and power loss of a transistor bank regulator.

It presents some practical problems, however. The leakage inductance and lead inductance at L1/L2 must be minimized in order to minimize the capacitor voltage and the resulting capacitor losses due to two voltage reversals per cycle. Operation at audio frequencies at this power level can produce objectional mechanical effects which must be dealt with. Also, the electrical interference generated causes difficulties, not the least of which is interference in the sensing of the current by the DCCT. Nevertheless, these are problems which can be solved, making this SCR chopper regulator a very interesting and useful alternate to more classical accelerator magnet power supply approaches.

## REFERENCES

1. E. M. Rowe and J. H. Weaver, "The Uses of Synchrotron Radiation", Scientific American, Vol. 236, #6, pp. 32-41. (June 1977).

2. R. E. Watson and M. L. Perlman, "Seeing with a New Light:Synchrotron Radiation", Science, 199, pp. 1295-1302. (March 1978).

3. S. B. Dewan and A. Straughen, "Power Semiconductor Circuits", John Wiley & Sons, 1975. pp. 298-318

4. L. T. Jackson, "P.E.P. Magnet Power Supply Systems", IEEE Transactions on Nuclear Science Vol. NS-24, No. 3, June 1977. pp. 1245-7.

CAPTIONS

Figure 1.   Chopper Control Loop
            NSLS Dipole Magnet Power

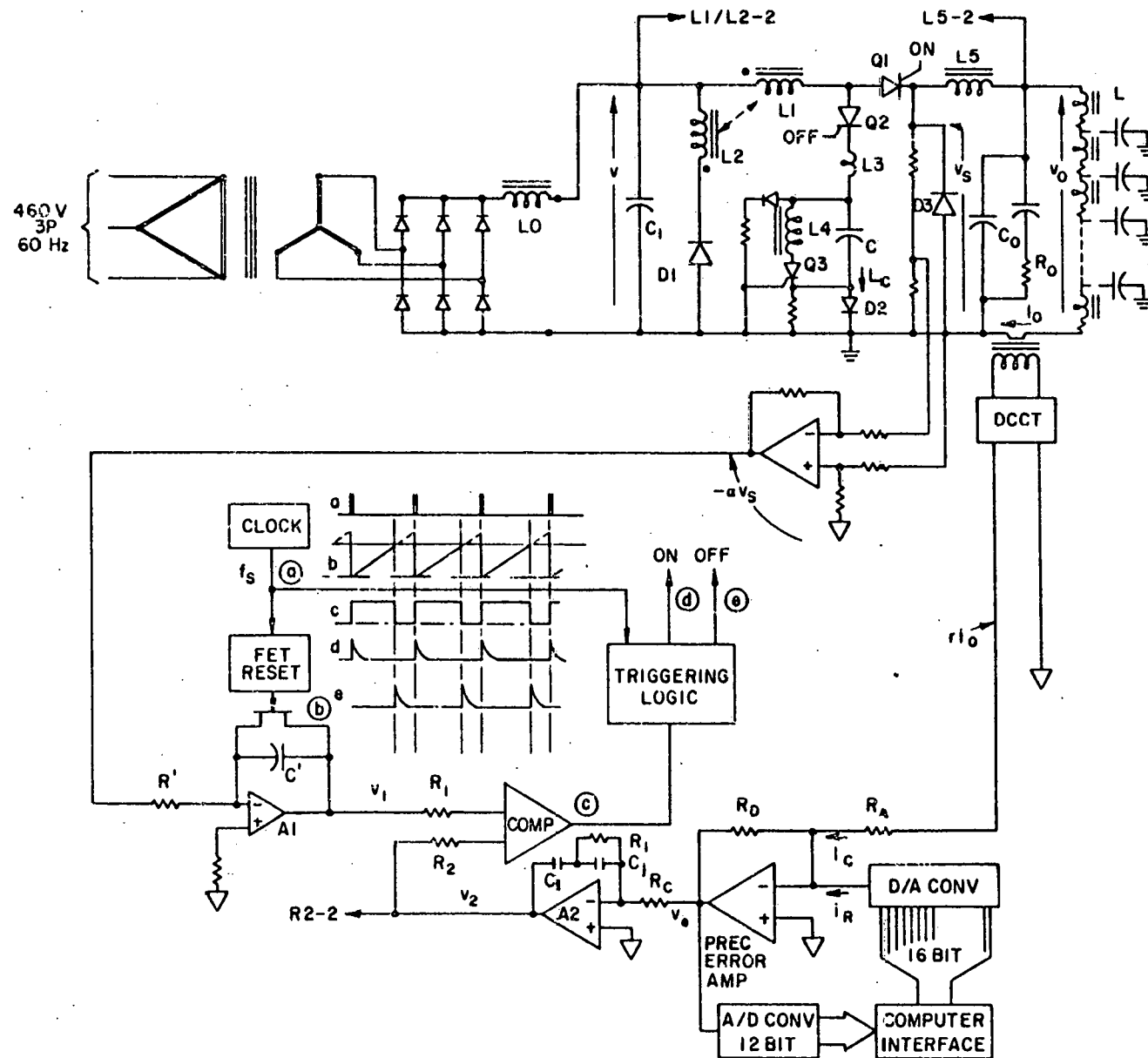
Figure 2a.  Chopper Switch Equivalent


Figure 2b.  Typical Waveforms $L_1 = L_2$ M


Figure 3.   Chopper Power Supply
            Block Diagram


Figure 4.   Frequency Response
            NSLS Dipole Power Source
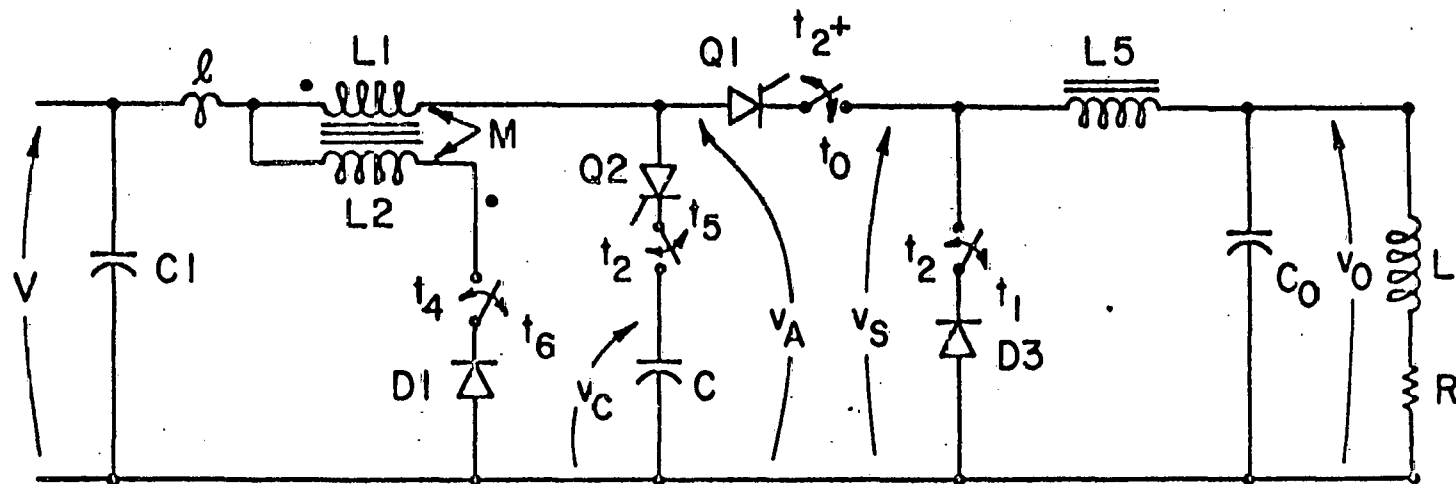

Figure 5.   Switch Assembly
            NSLS UV Dipole Power Source


Figure 6.   Switch Assembly Semiconductor
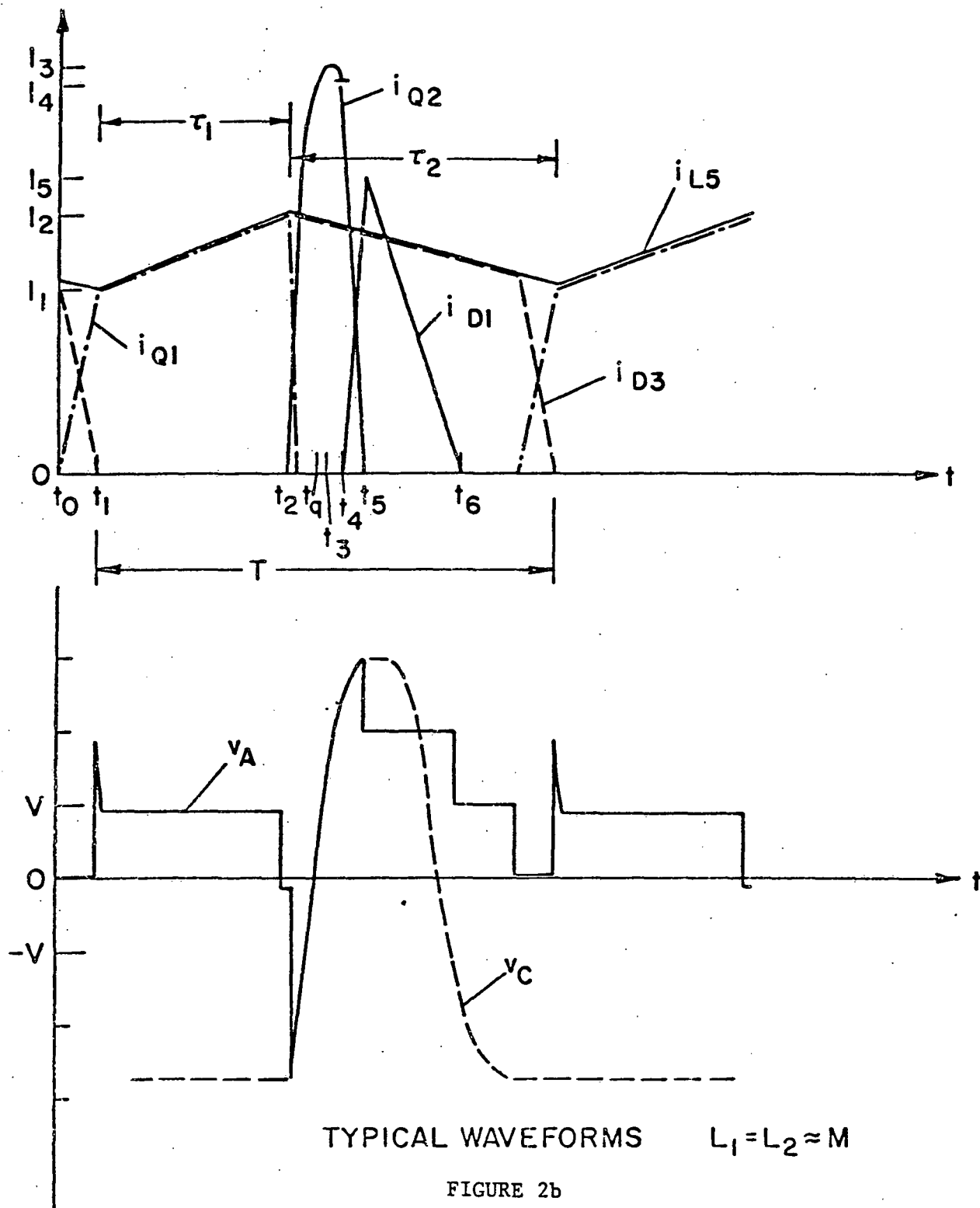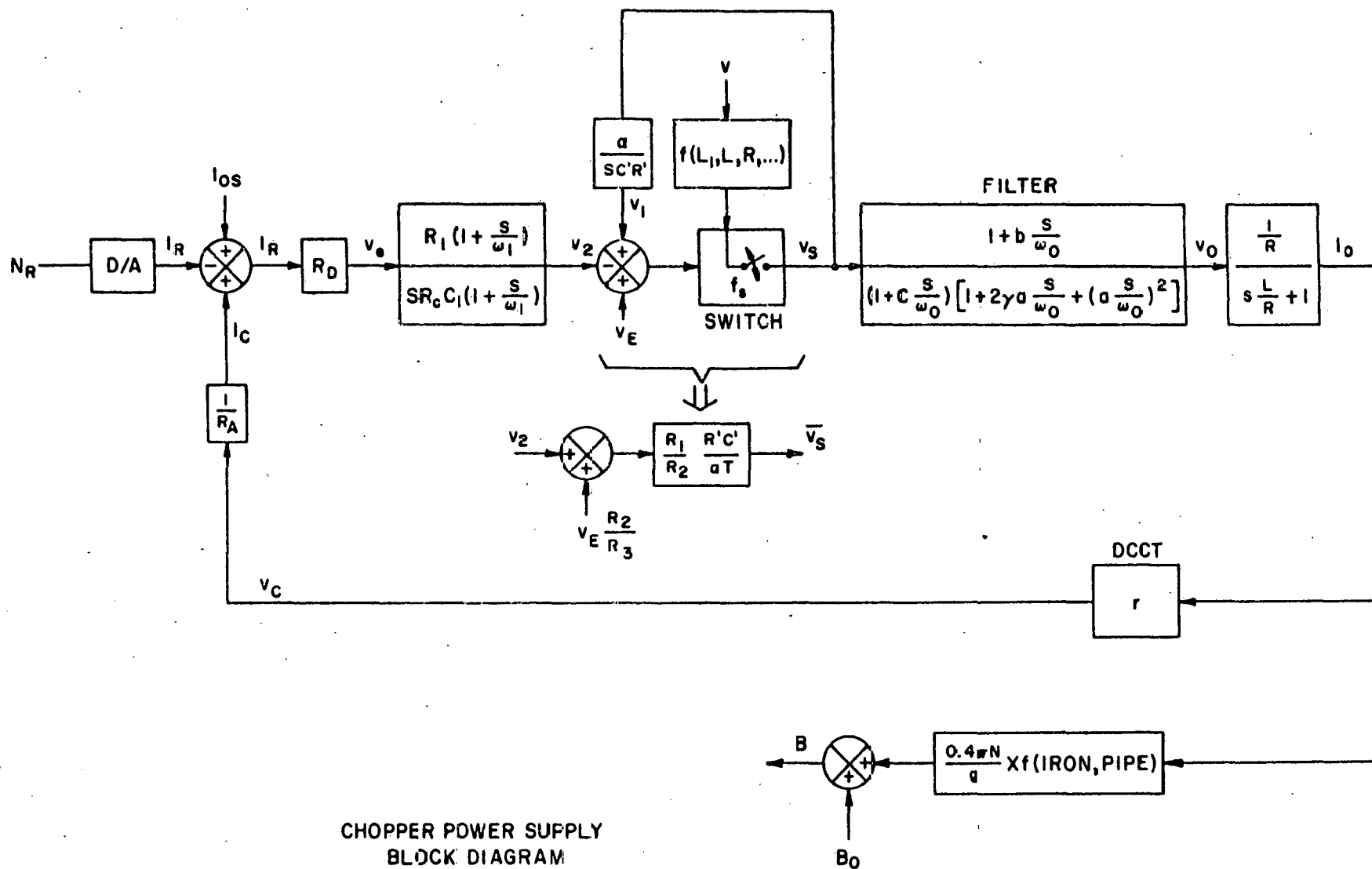            Components
            NSLS UV Dipole Power Source

CHOPPER CONTROL LOOP
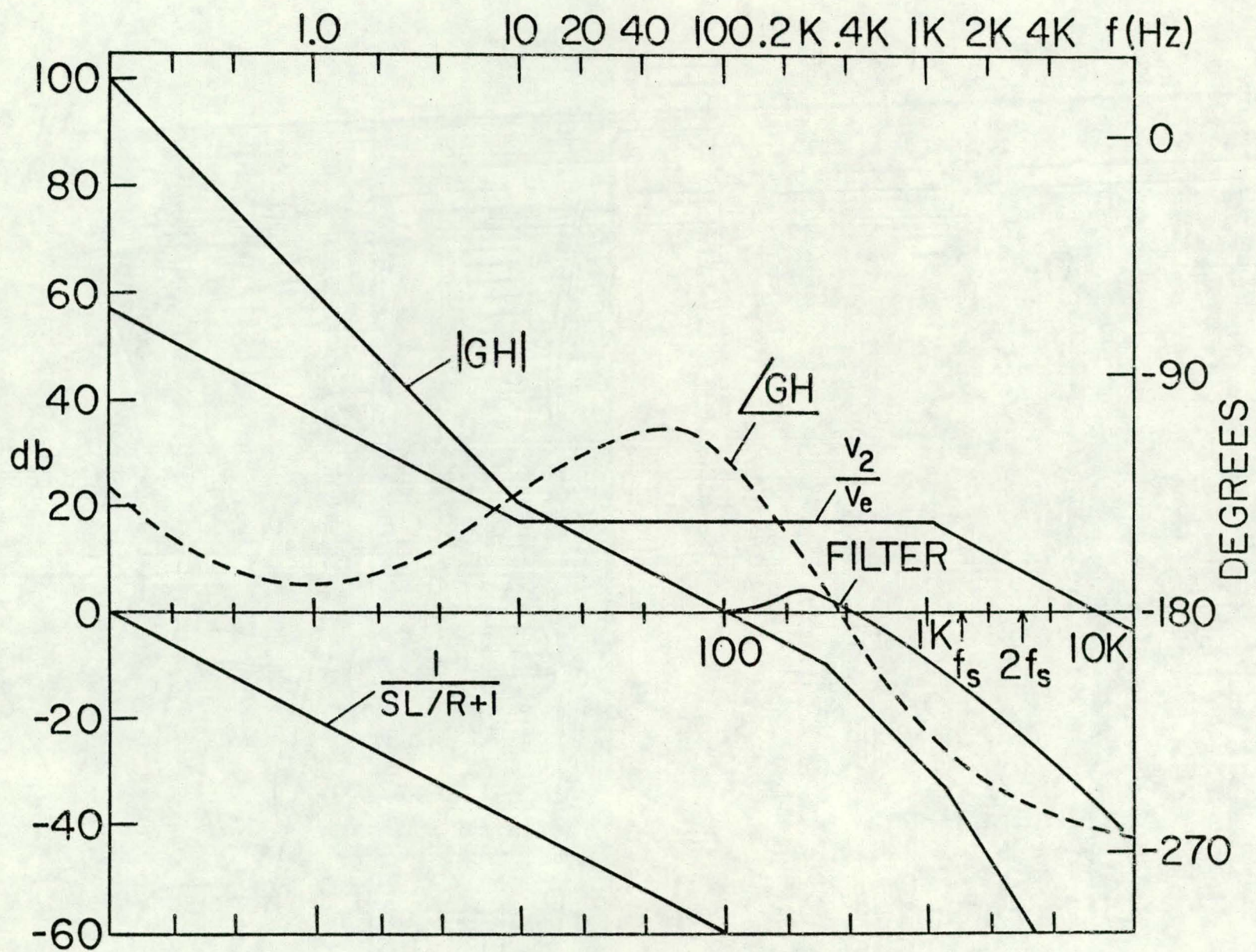NSLS DIPOLE MAGNET PWR
FIGURE 1

# FIGURE 2ₐ



CHOPPER SWITCH EQUIVALENT

TYPICAL WAVEFORMS $L_1 = L_2 \approx M$

FIGURE 2b

$N_R$ — D/A — $I_R$ — (⊕) — $I_R$ — $R_D$ — $v_e$ — box: $\dfrac{R_1\left(1+\dfrac{S}{\omega_1}\right)}{SR_cC_1\left(1+\dfrac{S}{\omega_1}\right)}$ — $v_2$ — (⊕) — SWITCH — $v_S$ — FILTER — $v_O$ — $\dfrac{\frac{1}{R}}{s\frac{L}{R}+1}$ — $I_O$

$I_{OS}$

$I_C$

$\dfrac{1}{R_A}$

$\dfrac{a}{SC'R'}$ — $v_1$

$f(L_1,L,R,\ldots)$

$v$

$v_E$

SWITCH $f_s$

FILTER
$$\dfrac{1+b\dfrac{S}{\omega_O}}{\left(1+c\dfrac{S}{\omega_O}\right)\left[1+2\gamma a\dfrac{S}{\omega_O}+\left(a\dfrac{S}{\omega_O}\right)^2\right]}$$

⇓

$v_2$ — (⊕) — $\dfrac{R_1}{R_2}\,\dfrac{R'C'}{aT}$ — $\overline{v_S}$

$v_E\dfrac{R_2}{R_3}$

DCCT
$r$

$v_C$

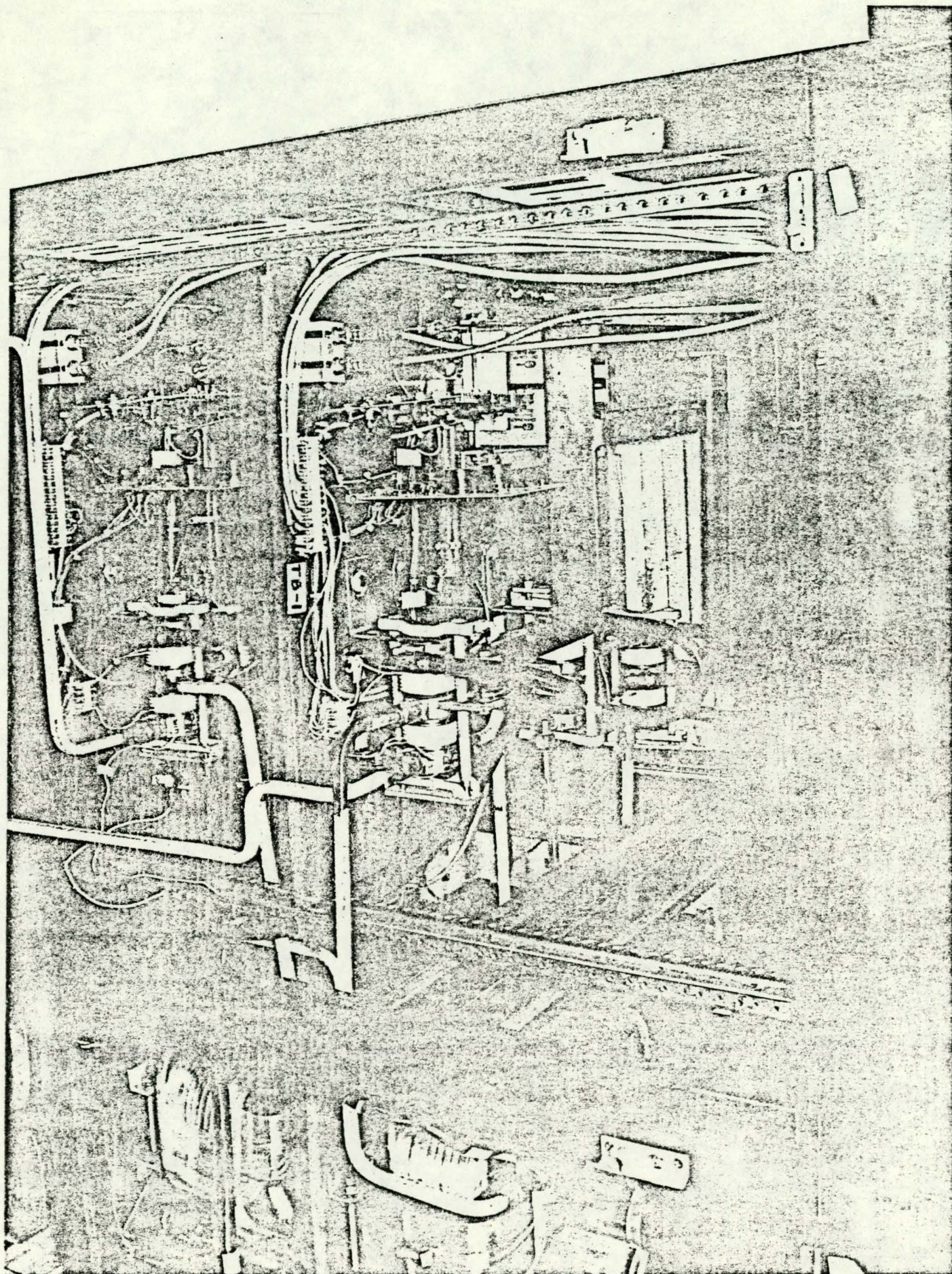$B$ — (⊗) — $\dfrac{0.4\pi N}{a}\,Xf(\text{IRON, PIPE})$

$B_O$

CHOPPER POWER SUPPLY
BLOCK DIAGRAM
FIGURE 3

FREQUENCY RESPONSE
NSLS DIPOLE POWER SOURCE
FIGURE 4

SWITCH ASSEMBLY
NSLS UV DIPOLE POWER SOURCE
FIGURE 5

SWITCH ASSEMBLY SEMICONDUCTOR COMPONENTS
NSLS UV DIPOLE POWER SOURCE
FIGURE 6